Muon transfer rates from hydrogen to ³He and ⁴He measured at low temperature

S. Tresch, R. Jacot-Guillarmod, F. Mulhauser, C. Piller, L. A. Schaller, L. Schellenberg, H. Schneuwly, Y.-A. Thalmann, and A. Werthmüller
Institut de Physique de l'Université, Pérolles, CH-1700 Fribourg, Switzerland

P. Ackerbauer, W. H. Breunlich, M. Cargnelli, B. Gartner, R. King, B. Lauss, J. Marton, W. Prymas, and J. Zmeskal
Institute for Medium Energy Physics, Austrian Academy of Sciences, A-1090 Wien, Austria

C. Petitjean
Paul Scherrer Institute, CH-5232 Villigen, Switzerland

D. Chatellard, J.-P. Egger, and E. Jeannet
Institut de Physique de l'Université, CH-2000 Neuchâtel, Switzerland

F. J. Hartmann and M. Mühlbauer
*Physik Department, TU München, D-85747 Garching, Germany*
(Received 17 October 1997)

The transfer reaction of negative muons from $(\mu p)_{1s}$ atoms to ³He and ⁴He was studied at 30 K, and the transfer rate to ³He was determined. Germanium detectors were employed to measure the time distribution of muonic neon x rays in triple-gas mixtures $H_2 + {}^{3,4}He + Ne$. The rates for the two helium isotopes, normalized to the atomic density of liquid hydrogen, are determined as $\lambda_{p^3He} = (0.29 \pm 0.12) \times 10^8$ s^{-1} and $\lambda_{p^4He} = (0.55 \pm 0.07) \times 10^8$ s^{-1}. The transfer rate to neon was obtained from binary $H_2 + Ne$ gas mixtures, measured at the same experimental conditions as for the triple-gas mixtures, with the result $\lambda_{pNe} = (0.0677 \pm 0.0032) \times 10^{11}$ s^{-1}. [S1050-2947(98)06604-9]

PACS number(s): 36.10.Dr, 34.70.+e, 82.30.Fi

I. INTRODUCTION

The charge-exchange process of negative muons from hydrogen isotopes to helium nuclei is important in muon-catalyzed fusion (μCF). Since helium is produced both in nuclear fusion reactions as well as in tritium decay, the helium atoms act as muon scavengers either by direct muon capture in helium or by muon transfer from hydrogen isotopes to helium nuclei, hence limiting the fusion yield.

Aside from its importance for μCF, the charge-exchange mechanism from muonic hydrogen isotopes to helium isotopes is interesting in itself. In contrast to elements with Z>3, where the direct ground-state transfer process

$$(\mu p)_{1s} + Z \rightarrow p + (\mu Z)^* \tag{1.1}$$
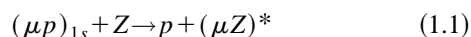
occurs generally with rates of the order of 10^{11} s^{-1}, direct transfer to helium isotopes occurs at a low rate of about $10^5 - 10^6$ s^{-1} [1,2] (the rates are normalized to the atomic density of liquid hydrogen). This is due to the absence of crossing and pseudocrossing points in the potential curves between the $\mu p + He^{2+}$ and the $p + (\mu He)^+$ system. In 1981, another transfer mechanism was proposed [3], namely, via the formation and decay of a metastable muonic hydrogen-helium molecule in the $(2p\sigma)$ excited state

$$(\mu p)_{1s} + He \rightarrow [(p\mu He)^* e^-]^+ + e^-. \tag{1.2}$$
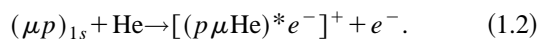
From this process, much higher transfer rates ($\sim 10^8$ s^{-1}) are expected. According to Ref. [3], the molecule should decay to the unbound $(1s\sigma)$ ground state with a rate of about 10^{12} s^{-1}, either by Auger effect or by a radiative transition emitting a ~ 7 keV x ray, leaving a hydrogen nucleus and a muonic helium atom in its ground state.

Several experiments measuring muon transfer from hydrogen to ⁴He were performed at room temperature, using different experimental methods. The triple-gas mixture method was employed in Refs. [4–6], with xenon or argon being the third gas. The analysis of the time distribution of the muonic xenon and argon x rays yielded transfer rates of the order of 10^8 s^{-1}, confirming indirectly the assumption of the molecular transfer process. However, the analysis of another experiment [7], measuring the x-ray yield of the radiative decay of the molecule in a binary $H_2 + {}^4He$ mixture, showed an order of magnitude lower transfer rate. This result was in disagreement with the theoretical calculations [3,8,9] and the other experimental results [4–6].

Several years later, the discrepancy between the lifetime and yield measurements could be explained [10] by the existence of a third decay channel, namely, the direct particle decay of the molecule, where the excess energy is shared between the hydrogen nucleus and the muonic helium atom. In addition, a strong isotopic dependence for this decay channel is predicted [10–15]: The rate decreases rapidly with increasing reduced mass of the two heavy particles. The observed strong isotopic dependence in the yield of the radiative decay of the respective molecules in liquid $D_2 + {}^3He$ and $D_2 + {}^4He$ targets [16] could indeed be explained by this decay channel. Including direct particle decay, the former discrepancy in the transfer rate λ_{p^4He} between the lifetime and the yield measurements also disappears [12].

The experimental situations for the transfer rates from hydrogen to ^{4}He and ^{3}He are quite different. For the ^{4}He case, several experimental values [4–7] exist, which are generally in agreement with theory. On the other hand, no experimental data are available for the muon transfer rate from hydrogen to ^{3}He. In addition, the theoretical predictions for ^{3}He vary considerably more than for ^{4}He (see Sec. V). Hence the main objective of the present experiment was the determination of the transfer rate from the ground state of the μp atom to ^{3}He. In order to achieve a high muon stop rate at low gas pressure, the experiment was performed at low temperature, around 30 K. The same method was also used to study the muon transfer rate to ^{4}He. Preliminary results of this experiment were communicated at the μCF conference at the Joint Institute for Nuclear Research (JINR) in Dubna [17].

II. EXPERIMENTAL METHOD

The muon transfer rates from hydrogen to ^{3}He and ^{4}He were determined using the triple gas mixture method, which was described in detail in Ref. [5]. This method is favored with respect to the direct observation of the 7-keV x rays from the radiative decay of the $(p\mu\text{He})^*$ molecules, because the x-ray yield is predicted to be only about 3–7 % [10–15]. The latter measurement would require long running times, while the triple-gas mixture method does not depend on the decay channels of the molecule. Indeed, the transfer rate to helium can be determined from the time distribution of the muonic x rays of the third gas component of higher Z. Since these muonic x rays are more energetic, they are more easily detectable. However, the triple-gas mixture method requires precise knowledge of both the muon transfer rate from hydrogen to the third gas component and the concentration of this component. The uncertainties of these quantities enter crucially into the final error of the transfer rate to helium.

In the present experiment, neon was chosen as the third gas component, because it remains gaseous under the given experimental conditions. In addition, the transfer rate from muonic hydrogen to neon is about one order of magnitude lower than that to other elements [18,19]. Therefore, a higher concentration of the third gas can be used, which in turn can be determined more accurately.

The kinetic processes in a triple-gas mixture of H$_2$+He+Ne, including a possible deuterium contamination, are displayed in Fig. 1. After the muon has reached the ground state $(\mu p)_{1s}$, it either decays with a rate $\lambda_0 = 4.5516 \times 10^5$ s^{-1} or forms a $pp\mu$ molecule with a rate $\lambda_{pp\mu}$, or transfers to helium $(\lambda_{p\text{He}})$, to neon $(\lambda_{p\text{Ne}})$, to deuterium (λ_{pd}), or to other impurities (λ_{pi}). The rates $\lambda_{p\text{He}}$, $\lambda_{pp\mu}$, $\lambda_{p\text{Ne}}$, λ_{pd}, and λ_{pi} are all normalized to the atomic liquid hydrogen density (LHD, 4.25×10^{22} atoms cm^{-3}). The total measured disappearance rate $\Lambda_{\mu p_{1s}}$ of the initially formed $(\mu p)_{1s}$ atoms can then be written as

$$\Lambda_{\mu p_{1s}} = \frac{1}{\tau_{\mu p_{1s}}} = \lambda_0 + \phi(c_{\text{He}}\lambda_{p\text{He}} + c_p\lambda_{pp\mu}$$

$$+ c_{\text{Ne}}\lambda_{p\text{Ne}} + c_d\lambda_{pd} + c_i\lambda_{pi}). \tag{2.1}$$

Here $\tau_{\mu p_{1s}}$ is the measured lifetime of the $(\mu p)_{1s}$ atom, ϕ is the atomic gas density relative to LHD, and c_j are the atomic
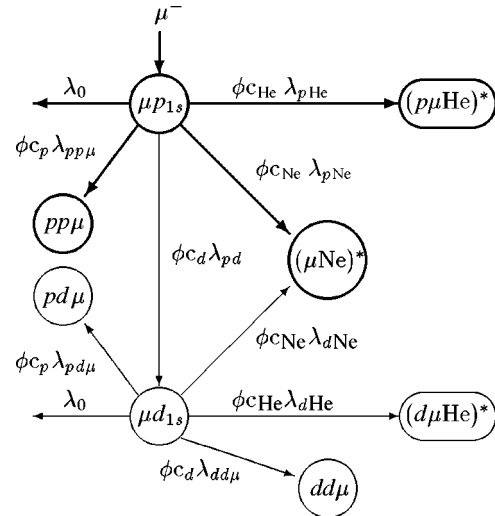

FIG. 1. Kinematics of the muon-induced processes in a triple-gas mixture H$_2$+He+Ne (bold). The starting point is the formation of a muonic hydrogen atom in the ground state $(\mu p)_{1s}$. The process chain in the presence of a deuterium contamination is also included.

gas concentrations of the j elements. The rates $\lambda_{pd} = (1.43 \pm 0.13) \times 10^{10}$ s^{-1} [20] and $\lambda_{pp\mu} = (2.34 \pm 0.17) \times 10^6$ s^{-1} [21] are used in this paper.

If the gas mixture is slightly contaminated by deuterium, direct atomic capture of the muon in deuterium can still be neglected, but not the formation of $(\mu d)_{1s}$ atoms by transfer from μp atoms. As a consequence, the muon is also transferred from muonic deuterium to helium and neon. The disappearance rate $\Lambda_{\mu d_{1s}}$ becomes, analogously to Eq. (2.1),

$$\Lambda_{\mu d_{1s}} = \frac{1}{\tau_{\mu d_{1s}}} = \lambda_0 + \phi(c_{\text{He}}\lambda_{d\text{He}} + c_{\text{Ne}}\lambda_{d\text{Ne}} + c_p\lambda_{pd\mu} + c_i\lambda_{di}),$$

$$\tag{2.2}$$

where $\lambda_{pd\mu} = (5.53 \pm 0.16) \times 10^6$ s^{-1} [21] is the normalized formation rate of $pd\mu$ molecules. At our experimental conditions, the $dd\mu$ formation rate [22] contributes less than 7 ppm, and is therefore omitted in Eq. (2.2).

Assuming that all transfer rates λ are energy independent, and that the $(\mu d)_{1s}$ atoms are only formed via transfer from the $(\mu p)_{1s}$ atoms, the time distribution of the muonic neon x rays, due to transfer from the ground state of muonic hydrogen and deuterium, can be written as

$$\frac{dN_{\gamma\text{Ne}}}{dt}(t) = N_0\phi c_{\text{Ne}}\left[\lambda_{p\text{Ne}}e^{-\Lambda_{\mu p_{1s}}t}\right.$$

$$\left. + \frac{\phi c_d\lambda_{d\text{Ne}}\lambda_{pd}}{\Lambda_{\mu d_{1s}} - \Lambda_{\mu p_{1s}}}(e^{-\Lambda_{\mu p_{1s}}t} - e^{-\Lambda_{\mu d_{1s}}t})\right],$$

$$\tag{2.3}$$

with N_0 the number of $(\mu p)_{1s}$ atoms formed at time zero. The disappearance rates $\Lambda_{\mu p_{1s}}$ and $\Lambda_{\mu d_{1s}}$ are obtained by fitting the measured time distribution of the muonic neon x rays. If the transfer to deuterium in the mixture is negligible,
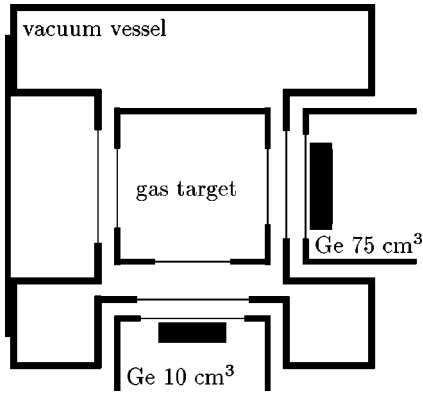
FIG. 2. Schematic front view of the target setup. The muons enter perpendicularly to the drawing. The thin lines represent target and detector windows, as described in the text.

the second term in the angular brackets of Eq. (2.3) vanishes and a simple exponential time distribution of the muonic neon x rays is expected. Given the muon transfer rate to neon, the muon transfer rate from hydrogen to helium can then be calculated using Eq. (2.1).

The transfer rate $\lambda_{p\mathrm{Ne}}$ has already been determined [18]. However, these measurements were performed at room temperature. In our triple-gas mixtures, the determination of $\lambda_{p\mathrm{He}}$ depends decisively on the precision of $\lambda_{p\mathrm{Ne}}$. Hence we measured this rate in binary H_2+Ne gas mixtures at ~30 K.

III. TARGET AND DETECTION SYSTEM

The experiments were performed at the μE4 channel of the ring accelerator of the Paul Scherrer Institute (PSI) in two run periods. Target and gas handling system [23,24] were optimized for low-temperature gas measurements around 30 K. The experimental setup is schematically presented in Fig. 2. The target cell was made from aluminum with outer dimensions of $6.5\times6.5\times11$ cm^3 and a total useful volume of about 250 cm^3. The ports, through which radiation could exit to the external detectors, were covered by thin hostaphan or kapton foils. The muon entrance window of the target cell was made of 75-μm kapton. Kapton foils covered also the windows of the vacuum vessel on the detectors sides. A 100-μm-thick aluminum foil was used for the muon beam entrance window.

Two germanium detectors with active volumes of 10 and 75 cm^3 were placed at an average distance of 8 cm from the target center. They covered the energy range of the Balmer and Lyman series of the muonic neon x rays (39–64 and

207–270 keV, respectively). The time resolutions were determined from the widths of the prompt muonic neon lines in a measurement with neon only. The time resolution of the 10-cm^3 detector was typically 12 ns for the Balmer and 7 ns for the Lyman series. The 75-cm^3 detector had a time resolution of 12 ns for the Lyman series.

The muon beam with a nominal momentum of 37.5 MeV/c was defined by a $6\times8.5\times0.1$ cm^3 plastic scintillator in anticoincidence with a second scintillator, which had an aperture of 4-cm diameter centered at the axis of the target. With a primary proton beam current of 1 mA and muon beam defining slits of 1.7×1.7 cm^2, around 13 000 muons/s entered the target. A pile up rejection circuit of ±9-μs gate length reduced the muon rate to 7500/s, resulting in a gated counting rate for the 10 and 75 cm^3 detectors of 180 and 650 counts/s, respectively. The energy signals were digitized in an analog-to-digital converter (ADC) and the time events in a time-to-digital converter (TDC) with a resolution of 1 ns per channel.

The gas mixture was obtained by filling the target vessel with the corresponding partial pressures of each gas component. The hydrogen gas was flushed through a palladium filter to remove impurities. For the second run, hydrogen with less than 20-ppm deuterium content was produced by electrolysis of deuterium depleted water. From a capillary leading directly into the target cell, several samples were taken before, during, and after the run, in order to monitor the stability of the concentrations. The samples were analyzed by a quadrupole mass spectrometer with high resolution.

The time distributions of the neon x rays were analyzed in four different gas mixtures: two binary H_2+Ne mixtures to determine the transfer rate to neon, one in each of the two run periods, and two triple mixtures to determine the transfer rate to the helium isotopes, namely, ^{3}He and ^{4}He. The characteristics of these mixtures are listed in Table I.

IV. RESULTS

A typical energy spectrum (prompt and delayed events) of the muonic Lyman series of neon is shown in Fig. 3. Due to the small percentage of neon in this mixture, the relative intensities of the lines are essentially determined by the structure of the delayed events. The four runs with binary- or triple-gas mixtures (see Table I) were all analyzed in the same way. In the first step, the time spectra were constructed by setting energy windows on the photopeaks of each of the muonic neon x rays having sufficient statistics, namely, the μNe(2–1), and the μNe(3–2) to μNe(5–2) lines for the 10-cm^3 detector, and the μNe(2–1) to μNe(5–1) lines for the 75-cm^3 detector. To subtract the background from these

TABLE I. Target characteristics of the gas mixtures. The mixtures (*A*) and (*C*) contained less than 20-ppm deuterium.

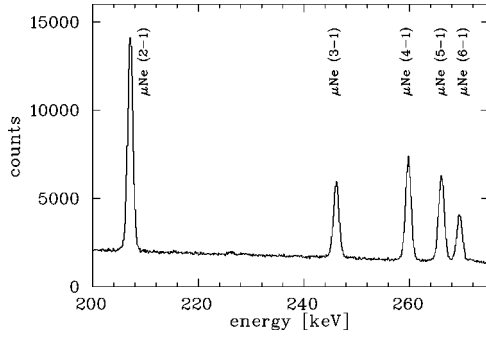|	Mixture: H_2 +					
Label	c_d (%)	c_{Ne} (%)	c_{He} (%)	Density ϕ (% of LHD)	Pressure (bar)	Temperature (K)
(*A*)	<0.002	0.65±0.03	0	7.39±0.07	4.56±0.01	27.5±0.2
(*B*)	0.055±0.01	0.24±0.01	0	5.50±0.05	3.72±0.01	27.8±0.2
(*C*)	<0.002	0.41±0.02	17.1±0.5 ^{3}He	7.33±0.11	5.56±0.01	26.0±0.2
(*D*)	0.035±0.007	0.33±0.01	36.4±0.6 ^{4}He	5.81±0.09	5.66±0.01	27.8±0.2

FIG. 3. Typical energy spectrum (prompt and delayed) of muonic neon x rays measured by the 75-cm^3 Ge detector in the H_2+^3He+Ne triple-gas mixture (C).

time spectra, events in the energy range below and above the respective x-ray lines were used. The $(\mu p)_{1s}$ lifetimes obtained from each of these spectra agreed with each other. Therefore, in a second step, all time spectra of a given run have been summed up. Before the final fit, the resulting time spectrum was compressed to 8 ns per bin. Since the transfer rate to neon must be known in our triple-gas measurement to determine the transfer rate to helium, it will be discussed first.

A. Transfer rate to Ne

Two measurements with binary mixtures (A) and (B) have been performed; see Table I. The time distribution of the delayed muonic neon x rays in mixture (A) shows a pure exponential decay [see Fig. 4(a)]. Hence, this time distribution was fitted by a single exponential function. The prompt peak, which is mainly due to direct muon capture in neon and excited-state transfer from muonic hydrogen to neon, was fitted by a Gaussian function. The lifetime obtained from the fit to the delayed part amounts to $\tau_{\mu p_{1s}}=257.7\pm1.0$ ns. With this value and the use of Eq. (2.1), the transfer rate from muonic hydrogen to neon is calculated as

$$\lambda_{p\mathrm{Ne}}=(0.0677\pm0.0003_{\mathrm{stat.}}\pm0.0032_{\mathrm{syst.}})\times10^{11}\ \mathrm{s}^{-1}.$$

This rate, measured at low temperature (~ 30 K), is clearly smaller than the one measured at room temperature, namely, $\lambda_{p\mathrm{Ne}}(300\ \mathrm{K})=(0.0849\pm0.0018)\times10^{11}\ \mathrm{s}^{-1}$ [18]. The systematical error will be discussed later.

The main difference of the binary mixture (B) compared to mixture (A), besides the different neon gas concentration, is the presence of 0.055% deuterium in the hydrogen gas, which was unexpectedly introduced by a deuterium-contaminated palladium filter. The triple mixture (D), measured during the same running period, was therefore also affected. Although such a deuterium contamination is low enough to neglect the contribution from direct muon capture in deuterium, $(\mu d)_{1s}$ atoms are formed with a high rate by transfer from $(\mu p)_{1s}$ atoms ($\lambda_{pd}=1.43\times10^{10}\ \mathrm{s}^{-1}$). As a consequence, the detected muonic neon x rays are not only due to the transfer $(\mu p)_{1s}+\mathrm{Ne}\rightarrow p+(\mu\mathrm{Ne})^*$, but also due to the two step transfer process $(\mu p)_{1s}+d\rightarrow p+(\mu d)_{1s}$ followed by $(\mu d)_{1s}+\mathrm{Ne}\rightarrow d+(\mu\mathrm{Ne})^*$; see Fig. 1. At the given experimental conditions, the lifetime $\tau_{\mu p_{1s}}$ is much longer than $\tau_{\mu d_{1s}}$. With a significant fraction (in our case
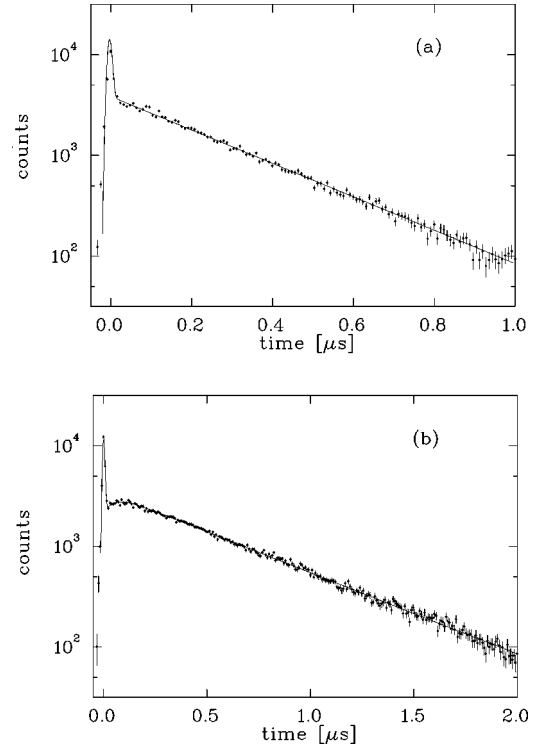

FIG. 4. Background-subtracted time spectra of the μNe x rays measured with the 10-cm^3 Ge detector. (a) shows a pure exponential decay of the x rays in the binary mixture (A). In (b), a deviation from the single exponential shape, due to a deuterium contamination in the binary mixture (B), is clearly seen.

45%) of muonic neon x rays due to transfer from $(\mu d)_{1s}$, one expects a deviation from a single exponential shape in the time distribution of the muonic neon x rays. This is indeed the case, as shown in Fig. 4(b) and described by Eq. (2.3). The spectrum was fitted using a Gaussian function for the prompt peak and two exponential functions for the delayed part. This allows to determine the lifetimes of both the $(\mu p)_{1s}$ and $(\mu d)_{1s}$ atoms, with the results $\tau_{\mu p_{1s}}=531.6\pm3.9$ ns and $\tau_{\mu d_{1s}}=52.2\pm7.8$ ns, respectively. With the help of Eq. (2.1), the transfer rate obtained from mixture (B) becomes then $\lambda_{p\mathrm{Ne}}=(0.0655\pm0.0011_{\mathrm{stat.}}\pm0.0071_{\mathrm{syst.}})\times10^{11}\ \mathrm{s}^{-1}$. This confirms the rate obtained from measurement (A) and corroborates at the same time a temperature effect in $\lambda_{p\mathrm{Ne}}$.

In both mixtures, the systematic error dominates the statistical one. The former encompasses the uncertainties of the gas concentrations, the gas density and the transfer rates other than to neon in Eq. (2.1). In mixture (A), the main contribution is due to the uncertainty of the neon gas concentration; in mixture (B), it is due to the uncertainty of the deuterium gas concentration. The rate $\lambda_{p\mathrm{Ne}}$, deduced from mixture (A), has a four times higher statistical precision and does not suffer from a deuterium contamination. Hence this value was used in the calculations to extract the transfer rates to helium from the measurements performed in the triple-gas mixtures.

As a special dividend, so to speak, the deuterium contaminated binary mixture (B) also yielded a transfer rate from muonic deuterium to neon with the result $\lambda_{d\mathrm{Ne}}=(1.39\pm0.20)\times10^{11}\ \mathrm{s}^{-1}$. This value is close to the result of a measure-
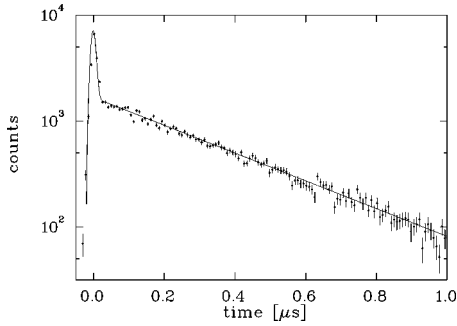
FIG. 5. Background-subtracted time spectrum of muonic neon x rays [sum of μNe(2–1), μNe(3–2) to μNe(5–2) transitions] measured by the 10-cm^3 Ge detector in the triple H$_2$ + ^{3}He + Ne mixture (*C*).

FIG. 6. Background-subtracted time spectrum of muonic neon x rays [sum of μNe(2–1), μNe(3–2) to μNe(5–2) transitions] measured by the 10-cm^3 Ge detector in the triple H$_2$ + ^{4}He + Ne mixture (*D*).

ment performed at room temperature, namely, $\lambda_{d\text{Ne}}(300 \text{ K}) = (1.010 \pm 0.026) \times 10^{11}$ s^{-1} [18].

B. Transfer rates to ^{3}He and ^{4}He

With the knowledge of the transfer rate to neon, the transfer rates to ^{3}He and ^{4}He can be extracted from the triple-gas mixtures (*C*) and (*D*). The time spectra of the neon x rays and the disappearance rate of the $(\mu p)_{1s}$ atoms were determined by the same procedure as for the binary mixtures.

The muon transfer rate from hydrogen to ^{3}He was obtained from the time distribution of the muonic neon x rays measured in the triple-gas mixture (*C*). This distribution can be reproduced by a single exponential function (see Fig. 5). A Gaussian function was added to fit the prompt events. The lifetime of the $(\mu p)_{1s}$ atoms was determined to be $\tau_{\mu p_{1s}} = 331.1 \pm 3.3$ ns and $\tau_{\mu p_{1s}} = 335.6 \pm 1.9$ ns for the 10- and 75-cm^3 detectors, respectively, yielding an average value of $\tau_{\mu p_{1s}} = 334.5 \pm 2.0$ ns. With Eq. (2.1), and using our experimentally obtained transfer rate to neon at ~ 30 K, the normalized transfer rate from muonic hydrogen to ^{3}He is obtained as

$$\lambda_{p^3\text{He}} = (0.29 \pm 0.02_{\text{stat.}} \pm 0.12_{\text{syst.}}) \times 10^8 \text{s}^{-1}.$$

This value is the first experimental determination of $\lambda_{p^3\text{He}}$, to our knowledge.

The transfer rate to ^{4}He was deduced from measurement (*D*). This mixture had a 0.035% deuterium contamination due to the same circumstances as in mixture (*B*). However, if we compare the time spectrum of the triple-gas mixture (*D*, Fig. 6) with the one of the binary mixture [*B*, Fig. 4(b)], no deviation from a single exponential shape is observed. The reason is the following: In the binary mixture (*B*), about 45% of the detected muonic neon x rays result from transfer of $(\mu d)_{1s}$ atoms to neon. In the triple-gas mixture, the contribution of these x rays to the total time spectrum is only 15%. Furthermore, due to the additional transfer to helium, the respective lifetimes of the $(\mu d)_{1s}$ atoms and $(\mu p)_{1s}$ atoms are smaller by about a factor of 2 than in the binary mixture. Due to the smaller number of muonic neon x rays after transfer from the $(\mu d)_{1s}$ atoms, together with their short lifetime of about 20 ns, a deviation from a single exponential function in the time distribution of the muonic neon x rays in the triple-gas mixture was not observed.
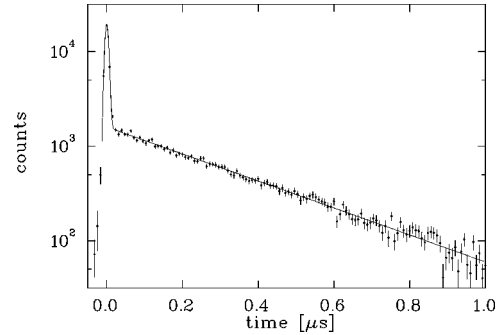
Hence, the delayed part of the time distribution in mixture (*D*) could be fitted with a single exponential function, yielding a lifetime of the $(\mu p)_{1s}$ atom of $\tau_{\mu p_{1s}} = 303.0 \pm 5.0$ ns. The normalized transfer rate from muonic hydrogen to ^{4}He becomes then, again using Eq. (2.1),

$$\lambda_{p^4\text{He}} = (0.55 \pm 0.03_{\text{stat.}} \pm 0.06_{\text{syst.}}) \times 10^8 \text{ s}^{-1}.$$

For both transfer rates to the two helium isotopes, the systematic errors dominate the statistical ones, as was already the case for neon. The main contribution to the systematic errors is the uncertainty of the transfer rate to neon, and in the case of ^{4}He also that of the deuterium contamination. In the ^{3}He mixture (*C*), the uncertainty in the neon gas concentration and the uncertainty in the transfer rate to neon influences the final error more than in the ^{4}He mixture (*D*). Due to the lower concentration of ^{3}He in (*C*) than of ^{4}He in (*D*), the helium term in Eq. (2.1) contributes only 12% to the total rate $\Lambda_{\mu p_{1s}}$ compared to 67% for the neon term. Therefore, a small change of 1% in the rate $\lambda_{p\text{Ne}}$ or in the neon gas concentration changes the transfer rate to helium by 6%. In the ^{4}He case, the helium and neon terms contribute both about equally (35%). Hence, a change in the neon term of 1% changes the helium term by the same amount.

V. CONCLUSION

In conclusion, muon transfer measurements have been performed at a low temperature of around 30 K. The transfer rate from the ground state of muonic hydrogen to ^{3}He has been measured. The transfer rate to neon, employed in these triple-gas mixtures, was redetermined in binary mixtures at ~ 30 K, and a 20% smaller rate was obtained than in similar measurements at 300 K.

Our results are compared to theoretical expectations and, in the case of $\lambda_{p^4\text{He}}$, also to experimental transfer rates (see Table II). A variety of theoretical calculations [3,8,9] using different approximations have been performed, yielding a certain range of values for both rates $\lambda_{p^3\text{He}}$ and $\lambda_{p^4\text{He}}$ at different temperatures. Comparing our experimental results with theory and other experiments [4–7] we arrive at the following conclusions:

(i) Our measured muon transfer rate from hydrogen to ^{3}He is smaller than any theoretical prediction. Depending on

TABLE II. Experimental and theoretical muon transfer rates from hydrogen to helium isotopes at ~ 30 and 300 K.

Rate	Temperature (K)	Mixture	Experiment (10^8 s^{-1})	Theory (10^8 s^{-1})	Reference
$\lambda_{p^3\text{He}}$	26	$H_2 + {}^3\text{He} + \text{Ne } (C)$	0.29 ± 0.12^a		this experiment
$\lambda_{p^3\text{He}}$	30			0.91	[3]
$\lambda_{p^3\text{He}}$	30			0.64	[8]
$\lambda_{p^3\text{He}}$	30			0.81–1.10	[9]
$\lambda_{p^4\text{He}}$	27.8	$H_2 + {}^4\text{He} + \text{Ne } (D)$	0.55 ± 0.07^a		this experiment
$\lambda_{p^4\text{He}}$	30			0.47	[3]
$\lambda_{p^4\text{He}}$	30			0.43	[8]
$\lambda_{p^4\text{He}}$	30			0.46–0.64	[9]
$\lambda_{p^4\text{He}}$	300	$H_2 + {}^4\text{He} + \text{Xe}$	0.36 ± 0.10		[4]
$\lambda_{p^4\text{He}}$	300	$H_2 + {}^4\text{He} + \text{Ar}$	0.51 ± 0.19		[5,6]
$\lambda_{p^4\text{He}}$	300	$H_2 + {}^4\text{He}$	0.44 ± 0.20^b		[7,12]
$\lambda_{p^4\text{He}}$	300			0.32–0.52	[3,8,9]

[a]The errors are rms errors of statistical and systematical uncertainties.

[b]This rate was corrected from the original work by taking into account the particle decay of the molecule.

the theoretical assumption used, the discrepancy amounts to a factor 2 to 4.

(ii) All three formerly measured muon transfer rates from hydrogen to ^{4}He at room temperature agree with each other, yielding an average value of $\lambda_{p^4\text{He}}(300 \text{ K}) = (0.40 \pm 0.08) \times 10^8 \text{ s}^{-1}$. Our rate, measured at low temperature (~ 30 K), is by about two standard deviations larger. A similar trend is seen in the theoretical predictions [3,8,9]. Contrary to the ^{3}He case, experiment and theory are in agreement. Nevertheless, the precision is not sufficient to distinguish between the different theoretical assumptions [3,8,9].

[1] S. S. Gershtein, Zh. Eksp. Teor. Fiz. **43**, 706 (1962) [Sov. Phys. JETP **16**, 501 (1963)].

[2] A. V. Matveenko and L. I. Ponomarev, Zh. Eksp. Teor. Fiz. **63**, 48 (1972) [Sov. Phys. JETP **36**, 24 (1973)].

[3] Y. A. Aristov *et al.*, Yad. Fiz. **33**, 1066 (1981) [Sov. J. Nucl. Phys. **33**, 564 (1981)].

[4] V. M. Bystritsky *et al.*, Zh. Eksp. Teor. Fiz. **84**, 1257 (1983) [Phys. At. Nucl. **57**, 728 (1983)].

[5] R. Jacot-Guillarmod *et al.*, Phys. Rev. A **38**, 6151 (1988).

[6] R. Jacot-Guillarmod *et al.*, Phys. Rev. A **55**, 3447 (1997).

[7] H. P. von Arb *et al.*, Muon Catal. Fusion **4**, 61 (1989).

[8] V. K. Ivanov *et al.*, Zh. Eksp. Teor. Fiz. **91**, 358 (1986) [Sov. Phys. JETP **64**, 210 (1986)].

[9] A. V. Kravtsov, A. I. Mikhailov, and N. P. Popov, J. Phys. B **19**, 2579 (1986).

[10] Y. Kino and M. Kamimura, Hyperfine Interact. **82**, 195 (1993).

[11] S. S. Gershtein and V. V. Gusev, Hyperfine Interact. **82**, 185 (1993).

[12] A. V. Kravtsov, A. I. Mikhailov, and V. I. Savichev, Hyperfine Interact. **82**, 205 (1993).

[13] V. I. Korobov, Hyperfine Interact. **101/102**, 329 (1996).

[14] V. B. Belyaev, O. I. Kartavtsev, V. I. Kochkin, and E. A. Kolganova, Hyperfine Interact. **101/102**, 359 (1996).

[15] V. Belyaev, O. Kartavtsev, V. Kochkin, and E. A. Kolganova, Z. Phys. D **41**, 239 (1997).

[16] K. Ishida *et al.*, Hyperfine Interact. **82**, 111 (1993).

[17] S. Tresch *et al.*, Hyperfine Interact. **101/102**, 221 (1996).

[18] R. Jacot-Guillarmod, Phys. Rev. A **51**, 2179 (1995).

[19] L. Schellenberg, Muon Catal. Fusion **5/6**, 73 (1990).

[20] E. J. Bleser *et al.*, Phys. Rev. **132**, 2679 (1963).

[21] V. M. Bystritsky *et al.*, Zh. Eksp. Teor. Fiz. **70**, 1167 (1976) [Sov. Phys. JETP **43**, 606 (1976)].

[22] C. Petitjean *et al.*, Hyperfine Interact. **101/102**, 1 (1996).

[23] B. Gartner *et al.*, Hyperfine Interact. **101/102**, 249 (1996).

[24] B. Lauss *et al.*, Phys. Rev. Lett. **76**, 4693 (1996).